Size Distributions of Precipitation Particles in Frontal Clouds[1]

ROBERT A. HOUZE, JR., PETER V. HOBBS, PAUL H. HERZEGH AND DAVID B. PARSONS

Department of Atmospheric Sciences, University of Washington, Seattle 98195

(Manuscript received 12 June 1978, in final form 3 October 1978)

ABSTRACT

Measurements of the size spectra of precipitation particles have been made with Particle Measuring Systems probes aboard an aircraft flying through frontal clouds as part of the CYCLES (*Cyc*lonic *E*xtra-tropical *S*torms) PROJECT. These measurements were obtained while the aircraft flew through the clouds associated with mesoscale rainbands at temperatures ranging from −42 to +6°C. Particles $\gtrsim$1.5 mm in diameter closely follow an exponential size distribution. Above the melting level precipitation occurs mainly in the form of ice particles. In this region the mean particle size of the exponential distribution increases with increasing temperature, indicating that the ice particles grow as they drift downward. The variance of the exponential distribution also increases with increasing temperature above the melting level, indicating that the particles grow particularly well by collection as they fall at various speeds. Passage of the falling particles through the melting level is accompanied by a sudden decrease in the mean and variance of the exponential size distribution.

1. Introduction

In studies of the growth of precipitation, cloud modeling and radar meteorology, it is important to know the nature of the size distribution of the particles. Measurements of particle-size distributions have been made at ground level in rain (Marshall and Palmer, 1948; Geotis, 1968; Waldvogel, 1974), snow (Imai *et al.*, 1955; Gunn and Marshall, 1958; and hail (Douglas, 1964; Federer and Waldvogel, 1975). Many of these studies have been reviewed by Battan (1973). In general, they show that precipitation particle sizes are distributed according to the relation suggested by Marshall and Palmer (1948), i.e.,

$$N(D)=N_0\exp(-\lambda D), \tag{1}$$

where $N(D)dD$ is the number of particles per unit volume of air with diameters between D and $D+dD$, and N_0 and λ are constants. In certain special cases, important deviations from the Marshall-Palmer (MP) distribution[2] have been noted (e.g., Mason and Andrews, 1960). However, the studies cited above indicate that in most situations, the MP distribution is a good approximation to the size distribution of precipitation particles at ground level for $D\gtrsim 1$ mm.

Measurements of the size distributions of precipitation particles above ground level are more scarce. Airborne measurements using an optical particle spectrometer indicate that precipitation-sized ice particles in cirrus clouds are distributed according to the MP form (Heymsfield and Knollenberg, 1972). In tropical clouds airborne foil impactor measurements suggest that both raindrops (Merceret, 1974a,b; Cunning and Sax, 1977) and precipitation-sized ice particles (Simpson and Wiggert, 1971) are distributed according to the MP distribution aloft. These results have important implications for cloud modeling, for the validity of (1) above ground level would justify the use of a microphysical parameterization scheme, such as first proposed by Kessler (1969), in which explicit calculation of the evolution of particle-size spectra is avoided by assuming that precipitation-sized particles are distributed according to (1) at all altitudes.

We are particularly interested in whether the MP distribution holds aloft in the frontal clouds which we are investigating as part of the CYCLES (*Cyc*lonic *E*xtratropical *S*torms) PROJECT. If it does, then future efforts to model these cloud systems may be justified in assuming a microphysical parameterization scheme based on (1). In this paper, we present and analyze airborne measurements of the size spectra of precipitation particles in frontal clouds obtained during the CYCLES PROJECT. These measurements are quite extensive, covering virtually the full range of temperatures aloft in frontal clouds, and they should be more precise than the foil impactor data of most earlier airborne studies.

[1] Contribution No. 465, Department of Atmospheric Sciences, University of Washington.

[2] We use the terminology MP distribution to refer to any particle size distribution described by (1), that is, any exponential distribution. We do not require that N_0 and λ have the particular values found by Marshall and Palmer.

0022-4928/79/010156-07$05.75

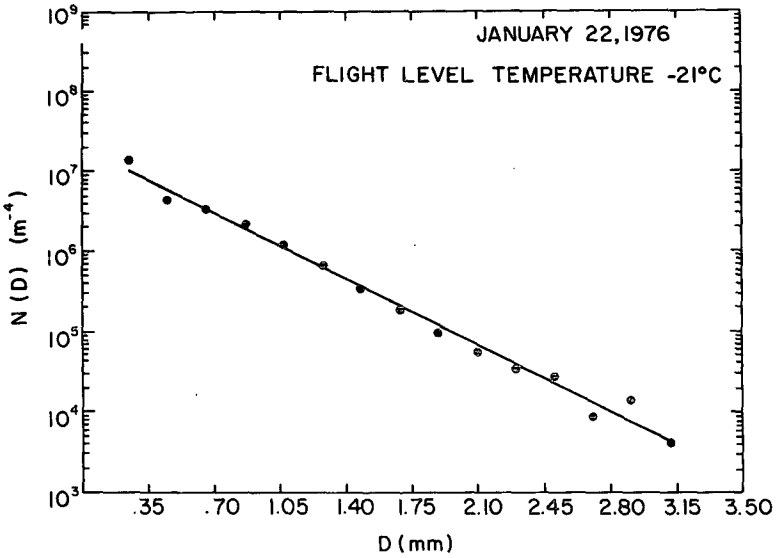

FIG. 1. Example of a measured particle-size spectrum which shows no significant deviation from a Marshall-Palmer distribution. $N(D)$ is the concentration of particles per unit interval of diameter D. The Marshall-Palmer distribution best fitting the data is estimated by the indicated straight line which was computed by the method of least squares.

2. Instrumentation and calibration procedures

Particle-size distributions were measured using a Particle Measuring Systems (PMS) cloud probe and a PMS precipitation probe (Knollenberg, 1970; Heymsfield, 1976) aboard the National Center for Atmospheric Research's Sabreliner aircraft. The PMS probes automatically count the numbers of sampled particles whose diameters fall within each of 15 size groups. The size groups for aggregate snow particles, which comprise most of the size spectra discussed here, range from 30 to 380 μm in the precipitation probe. These sizes reflect a slight adjustment over nominal values, in order to correct for the probe's response to the irregular shapes of aggregate snow (Knollenberg, 1975).

Proper sizing of the sampled particles was checked by frequent instrument calibrations in which glass

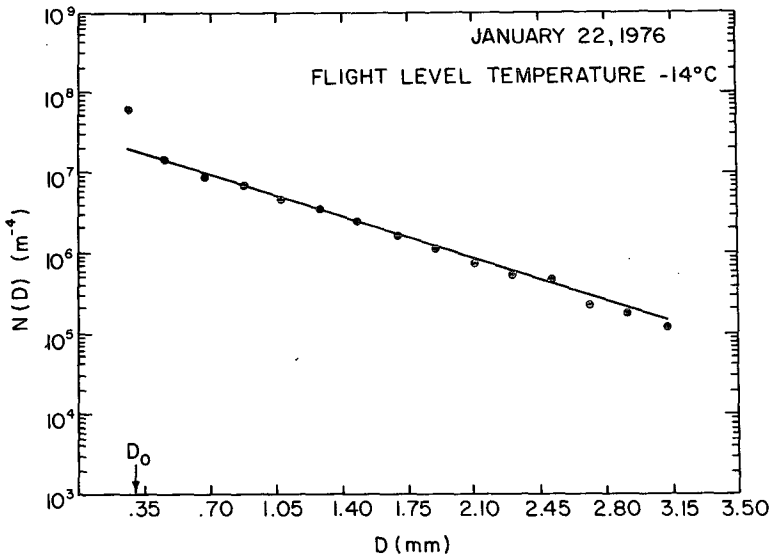

FIG. 2. Example of a measured particle-size spectrum which shows an enhanced type of deviation from a Marshall-Palmer distribution for diameters $D<D_0$. The Marshall-Palmer distribution best fitting the data for diameters $D\geq D_0$ is estimated by the indicated straight line which was computed by the method of least squares.

TABLE 1. Number of observed particle-size spectra which showed no deviation from an MP distribution, and the numbers exhibiting enhanced and suppressed types of deviations from an MP distribution for diameters $D<D_0$.

No deviation from MP distribution	Enhanced type of deviation	Suppressed type of deviation		
	D_0=0–0.4 mm	D_0=0.4–1.0 mm	D_0=1.0–1.5 mm	D_0=1.5–2.0 mm
9	13	6	9	1

and metal spheres of known diameters were blown through the sampling volumes of the PMS probes at high velocities, simulating in-flight sampling.

3. Synoptic and mesoscale situations in which the data were obtained

The data in this study were obtained in the clouds associated with one occluded front and three cold fronts. In each of these cases, the precipitation was concentrated in mesoscale rainbands (Houze *et al.*, 1976), and the Sabreliner flew along horizontal tracks at various altitudes back and forth through the clouds associated with the rainbands. The PMS data were averaged to produce one particle-size spectrum for each horizontal pass across a rainband. A total of 37 such spectra were obtained. The temperature at flight altitude during these passes ranged from −42 to +6°C.

4. Examples of particle-size distributions

Some of the measured particle-size spectra fit the MP distribution very closely over the entire sampled size range (Fig. 1). In other spectra, however, a truncated MP distribution was observed (Figs. 2 and 3). The latter spectra deviated from the MP form at the smaller particle end of the spectrum (that is, for diameters less than or equal to some threshold value D_0) but were described very accurately by the MP distribution for particles with $D \geqslant D_0$. Table 1 shows that D_0 exceeded 1.5 mm in only one case and never exceeded 2 mm. Table 1 also indicates that two types of deviations occurred. The cases in which D_0 lay between 0 and 0.4 mm were characterized in the region $D<D_0$ by enhanced values of $N(D)$ compared to the MP distribution fitting the large-particle ($D \geqslant D_0$) part of the distribution (Fig. 2). The cases in which D_0 lay between 0.4 and 2.0 mm were characterized in most of the region $D<D_0$ by suppressed values of $N(D)$ compared to the MP distribution which fitted the large-particle part of the distribution (Fig. 3). Note further that this suppressed, rather flat, spectral region typically had a lower bound near D=0.35 mm. Below this lower bound $N(D)$ increased rapidly with decreasing diameter, and, as in the enhanced deviations discussed above, fre-

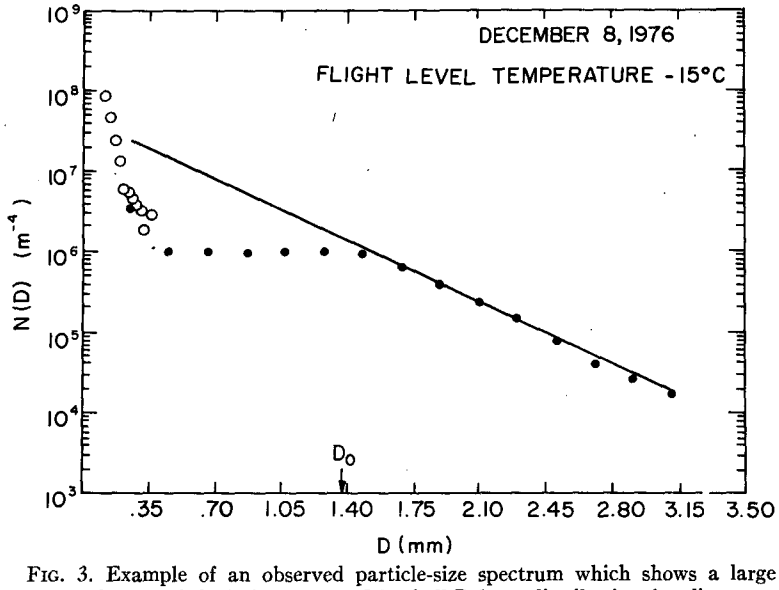

FIG. 3. Example of an observed particle-size spectrum which shows a large suppressed type of deviation from a Marshall-Palmer distribution for diameters $D<D_0$. The dark circles indicate data from the PMS precipitation probe, while the open circles indicate data from the PMS cloud probe. The Marshall-Palmer distribution best fitting the data for diameters $D \geqslant D_0$ is estimated by the indicated straight line which was computed by the method of least squares.

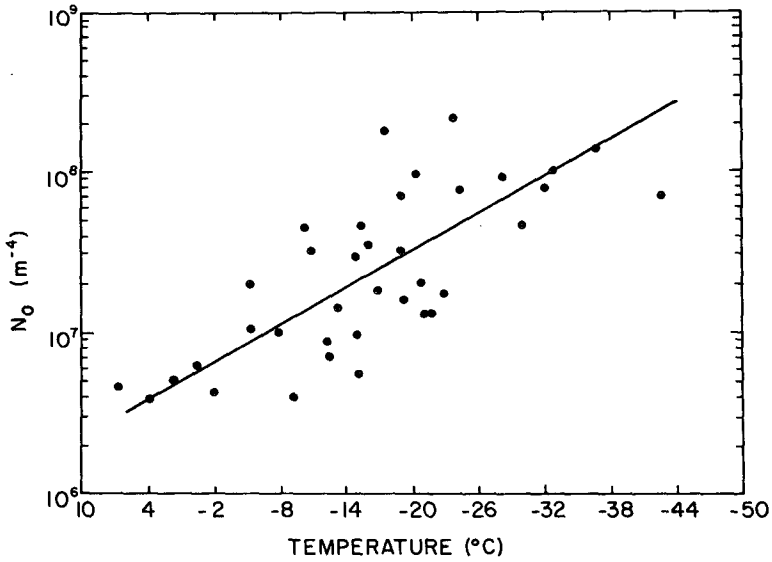

FIG. 4. Variation with temperature of the intercept parameter N_0 of the Marshall-Palmer distributions fitting the large-particle ($D \geqslant D_0$) part of all of the observed particle-size spectra. The best fit line computed by the method of least squares has a correlation coefficient of -0.66.

quently exceeded the values of $N(D)$ corresponding to the MP distribution which fitted the large-particle part of the distribution.

The reasons for the characteristic deviations from the MP spectrum at diameters $D<D_0$ in the truncated MP distributions, exemplified by Figs. 2 and 3, are not clear, but we find that such enhanced deviations at diameters $D<0.15$ mm are fairly common. These enhanced deviations may be associated with regions of cloud in which updrafts produce high concentrations of small liquid or ice particles. On the other hand, suppressed deviations are generally associated with broad distributions containing aggregated particles, and the suppression of particle concentrations at diameters $D<D_0$ frequently becomes stronger with increasing temperature. These facts suggest that suppressed deviations may be the result of collectional growth processes in which the concentrations of small and mid-sized particles are depleted through collection by larger particles. Suppressed deviations in raindrop distributions have been produced by the coalescence model of Srivastava (1971), and by the more detailed microphysical model of Yau and Austin (1979) which takes into account both warm and cold rain microphysics.

Whatever the reasons for the deviations in the small-particle part of the observed spectra, the data in the region of $D \geqslant D_0$ show an excellent fit to the MP distribution. This fact was checked by using the least-squares method to fit straight lines to the observed spectra, since the MP distribution is a straight line in log-linear plots such as those in Figs. 1–3. Best-fit straight lines were computed both for spectra showing no deviation from the MP distribution (Fig. 1) and for the data in the region $D \geqslant D_0$ of spectra showing enhanced or suppressed deviations from an MP distribution at $D<D_0$ (Figs. 2 and 3). In every case, the magnitude of the correlation coefficient for the best-fit line was >0.96.

Therefore, we conclude that each of the observed precipitation particle-size spectra was characterized by a basic MP distribution upon which other effects could be superimposed. In the smaller particle sizes, these other effects sometimes caused deviations from the form of the MP distribution, but the measured spectra always followed the MP form at diameters $D \geqslant D_0$. (We note that this result is consistent with the studies of particle-size spectra at ground level referred to in the Introduction; those studies showed the applicability of the MP distribution to surface precipitation only for $D \gtrsim 1$ mm.)

5. Variation of particle-size distribution parameters with temperature

We now examine the parameters N_0 and λ of the basic MP distributions characterizing the observed particle-size spectra. These parameters are indicated by the intercepts and slopes, respectively, of the computed straight lines described in Section 4. Although superimposed effects frequently led to a deviation from the basic MP distribution in the small particle-size range (Figs. 2 and 3), these effects did not prevent the basic MP spectra characterized by N_0 and λ from behaving in a systematic way. Figs. 4 and 5 show that at temperatures below 0°C, both

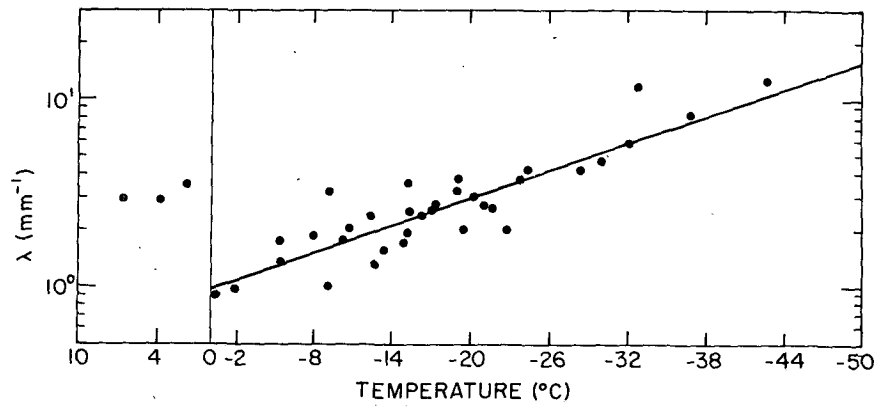

FIG. 5. Variation with temperature of the slope parameter λ of the Marshall-Palmer distributions fitting the large-particle ($D \geqslant D_0$) part of all of the observed particle-size spectra. The best-fit line computed for temperatures <0°C has a correlation coefficient of −0.90.

N_0 and λ decreased steadily toward higher temperatures. This corresponds to narrow particle-size spectra in the upper portions of frontal clouds evolving into much broader spectra at middle and lower levels. Note that Fig. 5 indicates a sudden increase in λ below the 0°C level. This corresponds to a narrowing in the particle-size distribution which occurs when aggregate snow particles melt to form much smaller, faster falling raindrops.

In order to understand further the variation with temperature of the observed particle-size distributions, it is useful to note that if (1) describes the size distribution of precipitation particles of diameter $D \geqslant D_0$, then for this size distribution the total number N_T of particles per unit volume of air is given by

$$N_T = \int_{D_0}^{\infty} N(D)dD = N_0\lambda^{-1}e^{-\lambda D_0}, \tag{2}$$

the mean diameter $\bar{D}$ of particles by

$$\bar{D} = N_T^{-1} \int_{D_0}^{\infty} D\,N(D)dD = D_0 + \lambda^{-1}, \tag{3}$$

the variance σ^2 of the diameters by

$$\sigma^2 = \overline{D^2} - \bar{D}^2 = N_T^{-1} \int_{D_0}^{\infty} D^2 N(D)dD - (D_0 + \lambda^{-1})^2 = \lambda^{-2}, \tag{4}$$

and the mass M of precipitation water per unit volume of air by

$$M = \int_{D_0}^{\infty} \rho\tfrac{1}{6}\pi D^3 N(D)dD = \rho\tfrac{1}{6}\pi N_0\lambda^{-4}e^{-\lambda D_0}(D_0^3\lambda^3 + 3D_0^2\lambda^2 + 6D_0\lambda + 6). \tag{5}$$

In (5) we assume that the particles are spherical and of density ρ.

Since the value of $\bar{D}$ in (3) is not affected by the high concentrations of small particles of $D < D_0$, changes in $\bar{D}$ can be interpreted as indicators of particle growth or evaporation at diameters $D \geqslant D_0$. Fig. 6 shows values of $\bar{D}$ calculated with a fixed D_0 equal to 1 mm. These values of $\bar{D}$ increase steadily with increasing temperature up to 0°C, at which temperature the values of $\bar{D}$ drop off discontinuously by about a factor of 0.6. This behavior is physically reasonable for a cloud in which ice particles form aloft at lower temperatures and grow as they drift downward toward regions of higher temperature. The mean particle diameter should increase with temperature until the particles reach the melting level. As explained in the next paragraph, we believe that the particles grow particularly effectively by collectional processes (riming or aggregation), although diffusional growth may also be significant. Passage through the melting level should be reflected as a sudden reduction in the mean particle size as the larger ice particles form smaller raindrops.

As the value of $\bar{D}$ increases with increasing temperature above the melting level, so does the variance σ^2 of the spectrum, given by λ^{-2} in (4). It is generally known that collectional growth processes lead to considerable broadening of particle size distributions and thus to an increase in their variance. The strong increase in the variance with temperature, which we observe, thus indicates that collectional processes are particularly active, with the consequent broadening of the size distributions becoming more prominent as the ice particles drift downward toward the melting level. As the ice particles pass through the 0°C level and melt to form much smaller raindrops, their size spectrum narrows.

The values of N_T given by (2) for the observed spectra showed a considerable amount of scatter, but generally tended to increase with increasing temperature. Thus, growth processes within the frontal clouds

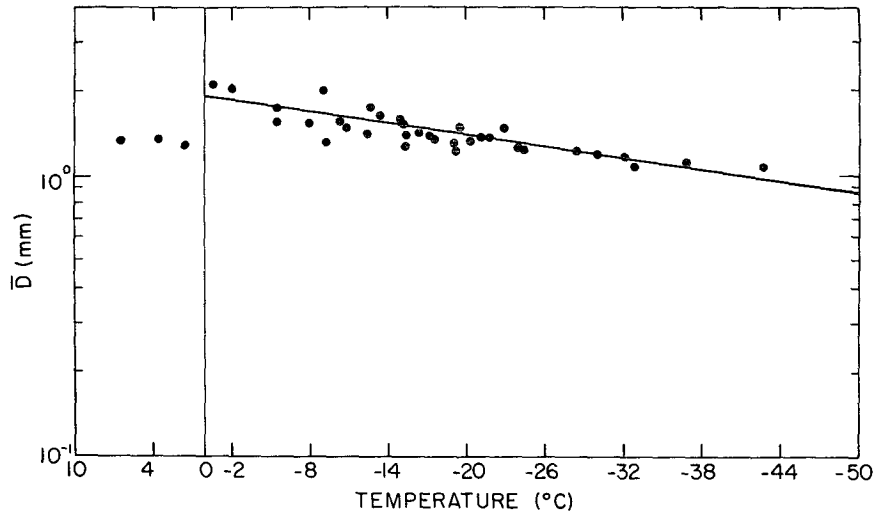

FIG. 6. Variation with temperature of the mean diameter $\bar{D}$ for particles of $D \geqslant 1$ mm. The best-fit line computed for temperatures <0°C has a correlation coefficient of 0.85.

led to increases in both the mean sizes and concentrations of precipitation particles in the range $D \geqslant 1$ mm.

The decrease of N_0 with increasing temperature (Fig. 4) has more scatter than the decrease of λ with increasing temperature above the melting level (Fig. 5). The reason for this scatter can be seen from (5), which indicates that N_0 is a function of both λ (which depends on T) and the total precipitation water content M in the MP distribution. From Fig. 7, the parameter N_0 is seen to increase with increasing values of M, and the magnitudes of the correlation coefficients corresponding to the four curves in Fig. 6 are all greater than or equal to the one obtained in the general plot of N_0 versus temperature in Fig. 5. Thus, the scatter in Fig. 5 is explained largely by the fact that M varied considerably from one spectrum to another.

6. Conclusions

As part of the CYCLES PROJECT, measurements of the size distributions of precipitation particles have been made aboard an aircraft flying through the clouds associated with mesoscale rainbands in midlatitude frontal systems at temperatures ranging from −42 to +6°C. The observed particle-size spectra tended to follow a basic MP distribution. Frequently, a deviation from this basic distribution occurred in the small-particle end of the observed spectra, but the basic MP form always dominated the spectra at diameters $\gtrsim 1.5$ mm. The mean particle diameter $\bar{D}$ in the range $D \geqslant 1$ mm and the variance (λ^{-2}) increased with increasing temperature above the melting level, while the parameters N_0 and λ decreased with increasing temperature. Crossing the melting level, from lower to higher temperatures, produced an abrupt decrease in the values of $\bar{D}$ and λ^{-2}.

We conclude from this study that in extratropical cyclonic storms the precipitation in clouds associated with mesoscale rainbands tends to originate as ice particles aloft. As these ice particles drift downward toward the melting level they grow, accounting for the increase in $\bar{D}$ with temperature above the 0°C level. Collection is apparently an important growth mechanism since the variance, or spread, of the MP distribution (indicated by λ^{-2}) also increases strongly with temperature above the melting level.

Passage of the precipitating particles through the melting level is accompanied by a sharp decrease in the mean particle size and spread of the basic MP distribution.

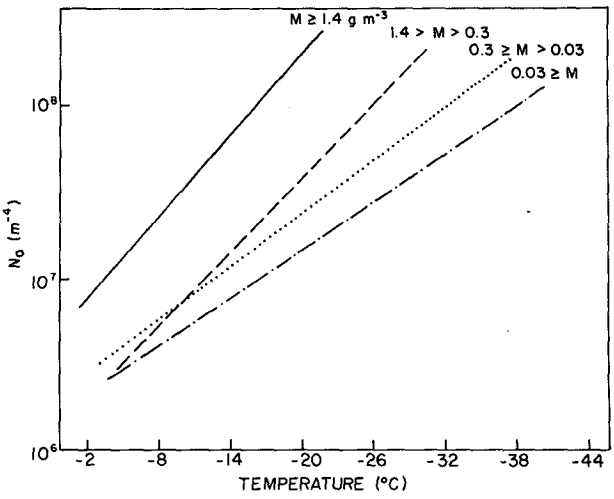

FIG. 7. Best-fit lines for N_0 obtained after subdividing the spectra according to the precipitation water content of the MP distributions associated with the observed particle-size spectra. Correlation coefficients for the four lines, in descending order of the indicated values of M, are −0.89, −0.66, −0.82 and −0.93.

The tendency of precipitation and particles in the clouds associated with frontal rainbands to follow the MP size distribution over a wide range of temperatures aloft has important implications for future attempts to model these cloud systems. Parameterizations of cloud microphysics, which assume an MP distribution in order to avoid explicit calculation of particle-size distributions, appear now to have an empirical basis. Such parameterizations may well be essential to making tractable the problems of modeling complex frontal cloud systems.

Acknowledgments. This work was supported by the Meteorology Program of the Atmospheric Research Section of the National Science Foundation under Grants ATM74-14726A03 and ATM77-01344 and by the Air Force Office of Scientific Research under Grant F49620-77-C-0057.

We thank members of the Research Aircraft Facility of the National Center for Atmospheric Research, which is sponsored by the National Science Foundation, for their help in operating the Sabreliner in the CYCLES PROJECT.

REFERENCES

Battan, L. J., 1973: *Radar Observation of the Atmosphere.* University of Chicago Press, 324 pp.

Cunning, J. B., and R. I. Sax, 1977: A *Z-R* relationship for the GATE B-scale array. *Mon. Wea. Rev.*, **105**, 1330–1336.

Douglas, R. H., 1964: Hail size distribution. *Preprints 11th Weather Radar Conf.*, Boulder, Amer. Meteor. Soc., 146–149.

Federer, B., and A. Waldvogel, 1975: Hail and raindrop size distributions from a Swiss multicell storm. *J. Appl. Meteor.*, **14**, 91–97.

Geotis, S. G., 1968: Drop-size distributions in eastern Massachusetts. *Preprints 13th Radar Meteorology Conf.*, Montreal, Amer. Meteor. Soc., 154–157.

Gunn, K. L. S., and J. S. Marshall, 1958: The distribution with size of aggregate snowflakes. *J. Meteor.*, **15**, 452–461.

Heymsfield, A. J., 1976: Particle size distribution measurement: An evaluation of the Knollenberg optical array probes. *Atmos. Tech.*, **2**, 17–24.

——, and R. G. Knollenberg, 1972: Properties of cirrus generating cells. *J. Atmos. Sci.*, **29**, 1358–1366.

Houze, R. A., P. V. Hobbs, K. R. Biswas and W. M. Davis, 1976: Mesoscale rainbands in extratropical cyclones. *Mon. Wea. Rev.*, **104**, 868–878.

Imai, I., M. Fujiwara, I. Ichimura and Y. Toyama, 1955: Radar reflectivity of falling snow. *Pap. Meteor. Geophys.*, **6**, 130–139.

Kessler, E., 1969: *On the Distribution and Continuity of Water Substance in Atmospheric Circulations. Meteor. Monogr.*, No. 32, Amer. Meteor. Soc., 84 pp.

Knollenberg, R. G., 1970: The optical array: an alternative to scattering or extinction for airborne particle size determination. *J. Appl. Meteor.*, **9**, 86–103.

——, 1975: The response of optical array spectrometers to ice and snow: A study of probe size to crystal mass relationships. Sci. Rep. No. 1, SC175C0141-9875-001, Air Force Cambridge Research Labs., 70 pp.

Marshall, J. S., and W. McK. Palmer, 1948: The distribution of raindrops with size. *J. Meteor.*, **5**, 165–166.

Mason, B. J., and J. B. Andrews, 1960: Drop-size distribution from various types of rain. *Quart. J. Roy. Meteor. Soc.*, **86**, 346–353.

Merceret, F. J., 1974a: A note on the distribution of raindrop-size spectra in Tropical Storm Felice. *Meteor. Mag.*, **103**, 358–360.

——, 1974b: On the size distribution of raindrops in Hurricane Ginger. *Mon. Wea. Rev.*, **102**, 714–716.

Simpson, J. S., and V. Wiggert, 1971: 1968 Florida cumulus seeding experiment: Numerical model results. *Mon. Wea. Rev.*, **99**, 87–118.

Srivastava, R. C., 1971: Size distribution of raindrops generated by their breakup and coalescence. *J. Atmos. Sci.*, **28**, 410–415.

Waldvogel, A., 1974: The N_0 jump of raindrop spectra. *J. Atmos. Sci.*, **31**, 1067–1078.

Yau, M. K., and P. M. Austin, 1979: A model for hydrometeor growth and evolution of raindrop size spectra. *J. Atmos. Sci.*, **36** (in press).